S1. Model parameters

The parameters in the model are determined, partly by referencing values used by previous researchers in similar ecosystems, partly by calibration of the K34 site, and partly by local physical values.

Table S1. Model parameter table

Symbol	Units	Remark	Source	
ρ	(kg/m³)	air density Standard parameters		
g_{v}	(m/s)	vapor conductance of leaf or stem surface	K34 site fit value	
g_s	(mol/m ² /s)	stomatal conductance of gas	K34 site fit value	
$f_{\rm str}$	-	water stress factor	(Santos and Costa, 2004)	
$c_{ m str}$	-	water stress coefficient	K34 site fit value	
c_r	-	root profile factor	K34 site fit value	
f_{wet}	-	fraction of wet surface	(Pollard and Thompson, 1995)	
δ_{w}	(m)	thickness of water film on the surface	K34 site fit value	
$\rho_{\mathbf{w}}$	(kg/m^3)	water density	Standard parameters	
$f_{ m prec}$	-	structural factor for rain water interception	(Pollard and Thompson, 1995)	
λ	(MJ/kg)	volumetric latent heat of vaporization	Standard parameters	
c_p	(MJ/kg/C)	specific heat of air	Standard parameters	
k	-	von Karman's constant	(Gan and Liu, 2020)	
Z _m	(m)	height at which wind speed and humidity are measured	Site average data	
d	(m)	zero-plane displacement height	Site average data	
h	(m)	canopy height	Site average data	
$V_{m,25}$	(µmol/m²/s)	maximum catalytic capacity of Rubisco per unit leaf area at 25°C	(Gan and Liu, 2020)	
β	[µmol/CO ₂ /(µmol/PAR)]	initial slopes of the light response curve to assimilation rate	(Gan and Liu, 2020)	

α	[µmol/m²/s/(µmol/m²/s)]	initial slopes of the CO ₂ response curve to assimilation rate	(Gan and Liu, 2020)
I ₀	(µmol/m²/s)	photosynthetically active radiation	(Gan and Liu, 2020)
C_{a}	(µmol/mol)	CO ₂ concentration	(Gan and Liu, 2020)
f	-	soil evaporation fraction that varies from 0 to 1	(Morillas et al., 2013; Zhang et al., 2019)
S	-	canopy storage capacity	(Lloyd et al., 1988)
р	-	free throughfall coefficient	(Lloyd et al., 1988)
p _t	-	proportion of rain diverted to the trunks	(Lloyd et al., 1988)
S_{t}	-	evaporation storage capacity from trunks	(Cuartas et al., 2007; Lloyd et al., 1988)
P_{t}	-	fraction of incident rainfall that is diverted to the trunks	(Cuartas et al., 2007; Lloyd et al., 1988)
К	-	extinction coefficient	(Cuartas et al., 2007)

S2. Correspondence of remote sensing data to the sites

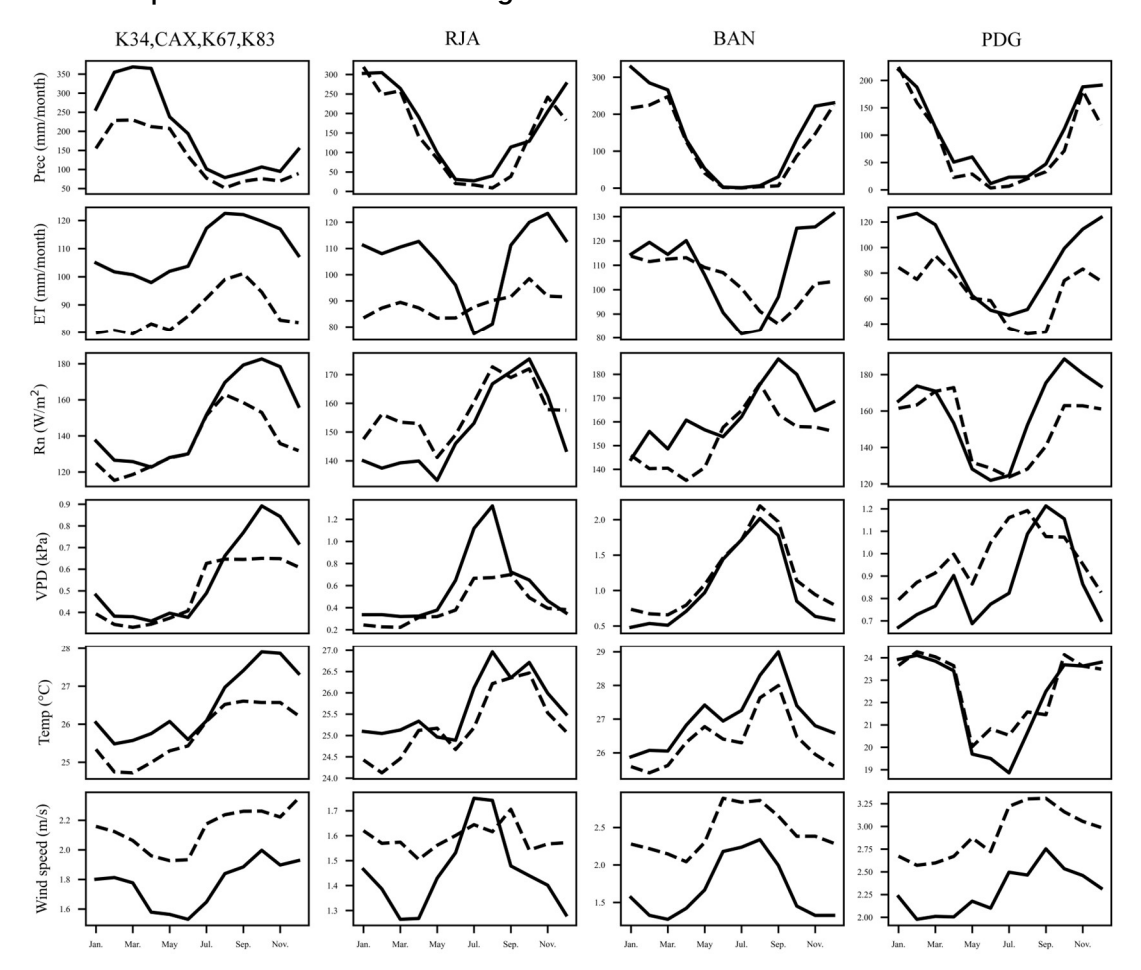


Fig. S1. Comparison of raster data with actual observations. The black dotted line represents the observations, and the solid black line represents the averaged raster data values

Due to the lack of locally measured LAI and NDVI data, we selected raster data corresponding to the latitude and longitude, and averaged several surrounding rasters to obtain the final data for use. To verify whether the averaged raster data corresponded to the stations, we also checked the correspondence of several other meteorological data (which had actual observational data). As shown in the figure, the meteorological data from the majority of stations exhibited consistent seasonality.

S3. Remove the analysis of the BAN site

Based on the simulation results from BAN, none of the three models can effectively capture the seasonality of ET. Therefore, to eliminate the potential errors that BAN may introduce in the summary analysis, we provide a summary analysis that excludes the results from the BAN site, with the aim of assessing whether the absence of BAN site results significantly alters the outcomes.

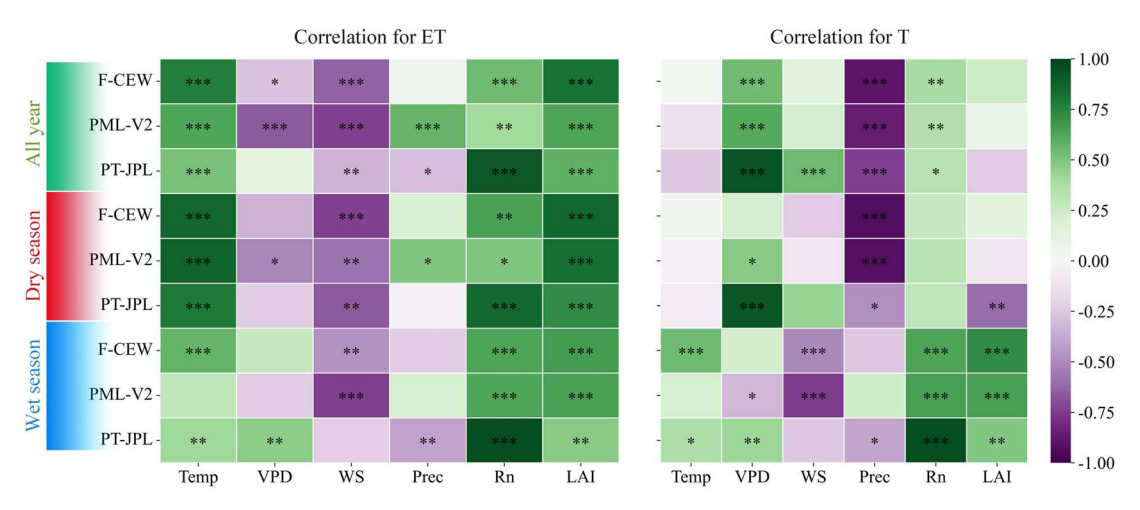


Fig. S2. The influence of environmental variables on ET and T, evaluating variables including temperature (Temp), vapor pressure deficit (VPD), wind speed (WS), precipitation (Prec), net radiation (Rn), and leaf area index (LAI). The table colors indicate Pearson correlation values, with left-hand side colors representing sampling periods (all seasons, dry season, and wet season).

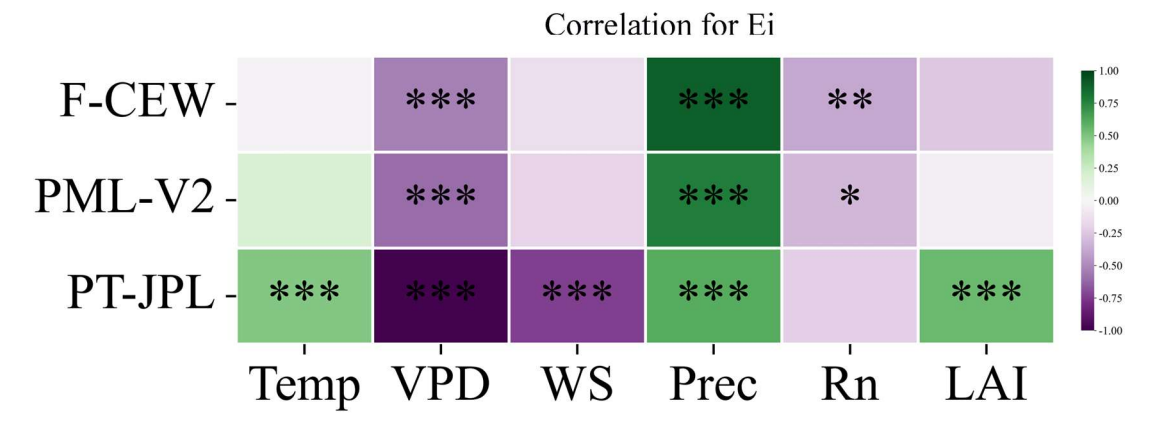


Fig. S3. The influence of environmental variables on Ei, evaluating variables including temperature (Temp), vapor pressure deficit (VPD), wind speed (WS), precipitation (Prec), net radiation (Rn), and leaf area index (LAI). The table colors indicate Pearson correlation values; * indicates significant correlation at P<0.05; ** at P<0.01; *** at P<0.001.

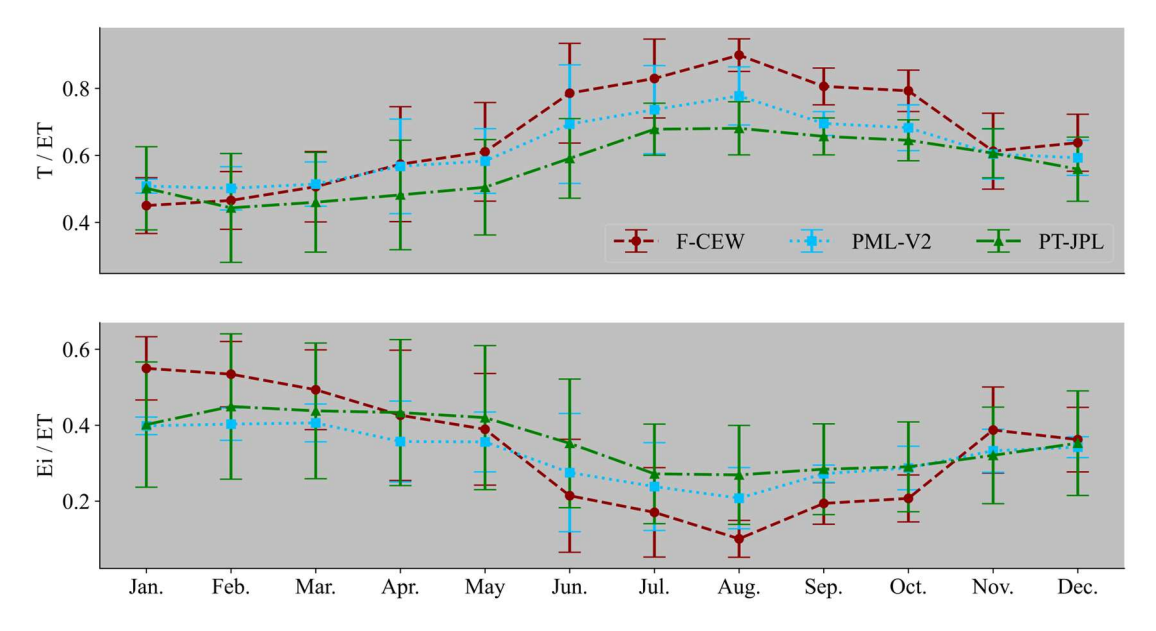


Fig. S4. The variability of T and Ei, with vertical lines in the chart indicating standard deviations.

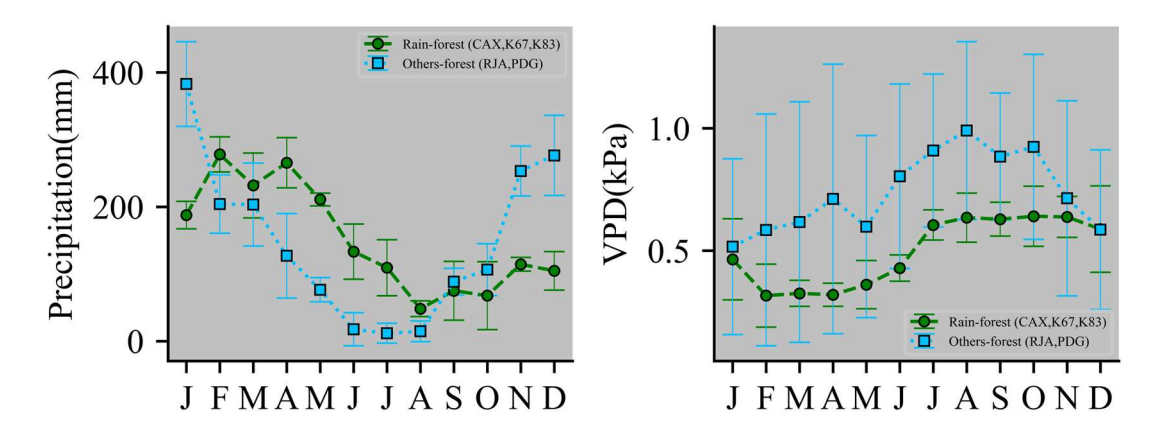


Fig. S5. The variability of precipitation and the variability of VPD, with vertical lines in the charts indicating standard deviations.

S4. Shorter time scale aggregation, no change in seasonality of ET

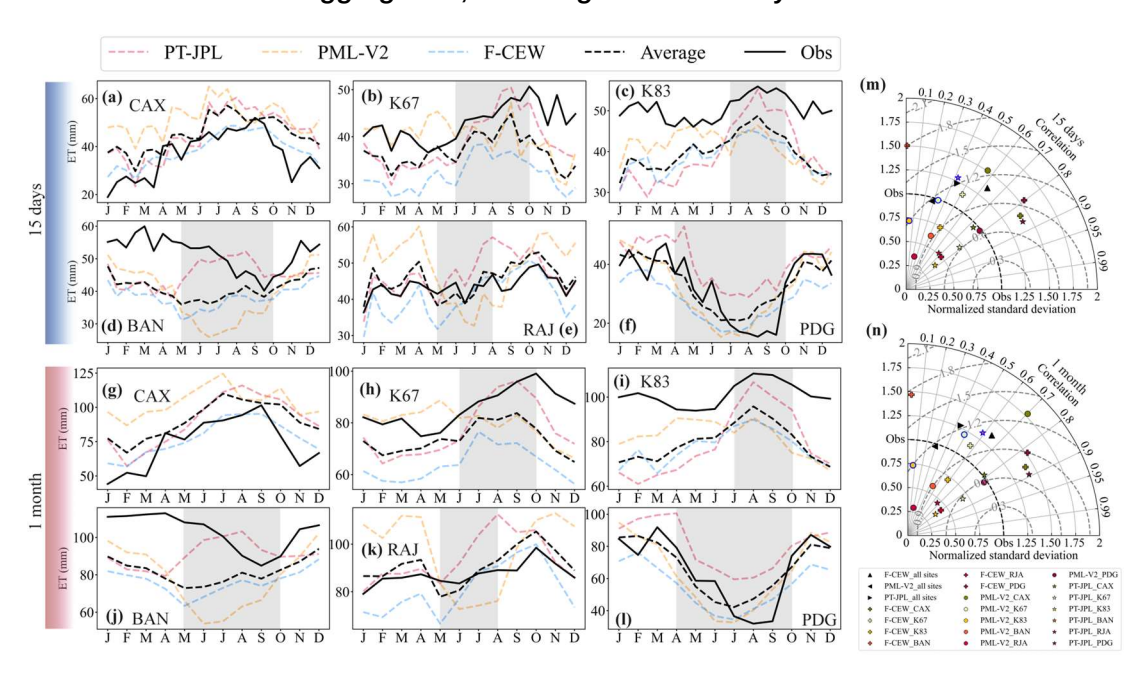


Fig. S6. (a-f) shows the results of 15 days time scale simulation, and (g-l) is 1 month time scale. Gray shaded areas indicate dry seasons, solid black lines represent observed ET values, and dashed black lines denote model averages; (m, n) is two time scale's Taylor diagrams respectively, providing a statistical summary of the models' seasonality against observed values. Blue-edged markers denote negative correlations, while black-edged markers indicate positive correlations. Black-filled triangles represent aggregated data from all sites, with different triangle orientations indicating different models: Forest-CEW (upward-pointing), PML-V2 (leftward-pointing), and PT-JPL (rightward-pointing). Colored filled markers represent individual sites, with shapes denoting different models: Forest-CEW (colored crosses), PML-V2 (colored circles), and PT-JPL (colored stars).

S5. Linear correlation of Ei and Es

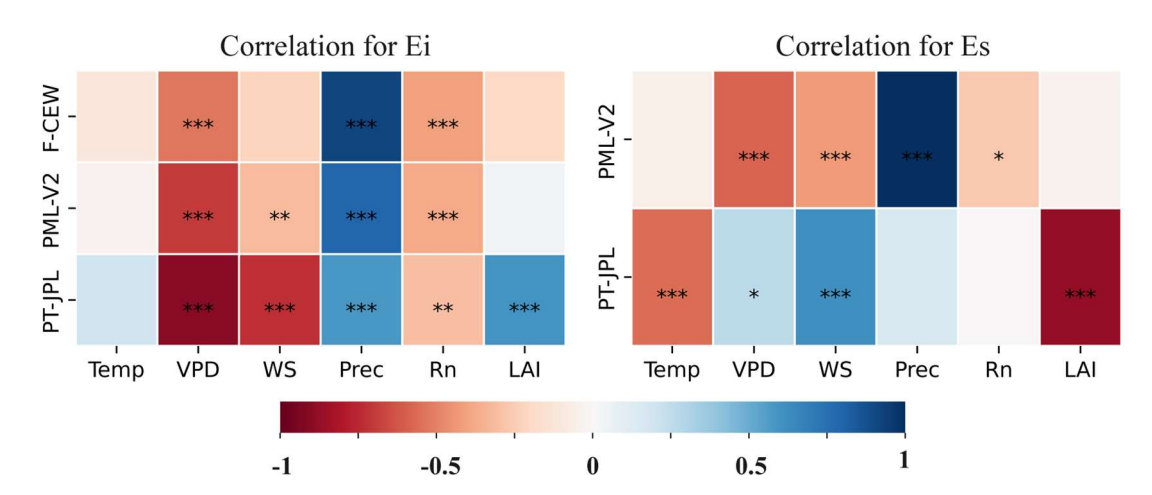


Fig. S7. Shows the influence of environmental variables on Ei and Es, evaluating variables including temperature (Temp), vapor pressure deficit (VPD), wind speed (WS), precipitation (Prec), net radiation (Rn), and leaf area index (LAI). The table colors indicate Pearson correlation values, and blue indicates a positive correlation, and red indicates a negative correlation; * indicates significant correlation at P<0.05; ** at P<0.01; *** at P<0.001.

We analyzed the drivers of the other two components. Canopy interception evaporation is mainly influenced by precipitation and VPD. However, after a precipitation event, the intercepted water on the leaves eventually returns to the atmosphere through evaporation, and the rate of this process is affected by environmental factors such as radiation, but the total amount of evaporation remains unchanged. The results of soil evaporation indicate that different models simulate this aspect differently. The PML-V2 model emphasizes precipitation as the main driver, while the PT-JPL model focuses on LAI. In reality, soil evaporation is a complex process, especially in forests, as it is not only a result of meteorological conditions but is also influenced by soil texture and structure. However, both models agree that there is no strong correlation between soil evaporation and radiation, because the dense canopy obstructs radiation from reaching the soil surface.

S6. Comparison of EI in ET with other EI models

To enhance model accuracy, we incorporated two classical Ei models: Rutter and Gash, as references. Ei plays a crucial role in the forest ET process, capturing rainfall in the plant canopy

and partially returning it to the atmosphere through evaporation. The Rutter model, proposed by Rutter (Rutter et al., 1971), describes the dynamic changes of Ei through detailed water balance equations. This model divides the interception process into three stages: rainfall, interception saturation, and drip, making it suitable for detailed instantaneous process studies.

In contrast, the Gash model, proposed by Gash (Gash et al., 1995), simplifies the description of Ei and is more suited for long-term average interception estimates. The Gash model statistically analyzes multiple rainfall events to determine the interception amount for each type of rainfall, calculating the interception volume by subtracting evaporation losses and drip amounts from total rainfall. While the Rutter model accurately simulates short-term interception dynamics, the Gash model is widely used for long-term interception estimates due to its simplicity and ease of parameterization.

S6.1 Rutter model

The Rutter model is a numerical model of rainfall interception based on the balance of water in the canopy and the trunk. Originally designed for Corsican pine forests in the United Kingdom, its application has expanded globally, with many forest types, including tropical forests (Lloyd et al., 1988; Schellekens et al., 1999). The model quantifies the amount of water stored in the canopy as the portion of rainfall that hits the canopy, the amount of water discharged from the canopy, and the amount of evaporation of the trapped water:

$$\frac{dc}{dt} = \begin{cases} (1 - p - p_t)R - E_w - D, & C \ge S\\ (1 - p - p_t)R - (\frac{c}{S})E_w - D, & C < S \end{cases}$$
 (1)

Where C(mm) is the amount of water on the canopy; R(mm/min) is the rainfall intensity; $E_w(mm/min)$ is the evaporation rate from the wet canopy; D(mm/min) is the drainage rate of water stored on the canopy; S, p, and p, represent the canopy storage capacity, the free throughfall

coefficient, and the proportion of rain diverted to the trunks (Lloyd et al., 1988). $E_{\rm w}$ uses the Penman-Monteith equation to calculate potential evaporation:

$$\lambda E_w = \frac{\Delta \cdot A + \rho \cdot C_p \cdot VPD/r_a}{\Delta + \gamma} \tag{2}$$

Where Δ , γ , VPD, ρ and C_p are the same as before; A is the net radiation (W/m²); r_a is the aerodynamic resistance, which can be calculated by:

$$r_a = \frac{\left(ln^{\frac{z_m - d}{z_{om}}}\right)^2}{k^2 u_m} \tag{3}$$

Where k, z_m , d, z_{om} and u_m are the same as in PML-V2.

D can be calculated by:

$$D = \begin{cases} D_0 \cdot \exp[b(C - S)], & C \ge S \\ 0, & C < S \end{cases}$$
 (4)

Where D_0 is the drainage rate (mm/min), D_0 =0.0018S; b is an empirical parameter, b=3.86S (Schellekens et al., 1999).

In this study, the set of equations for the Rutter model was approximated using the Eulerdifference method.

S6.2 Gash model

The Gash model is an effective method to study the interception process of precipitation in forest ecosystems, which is widely used in various forest types (Cuartas et al., 2007; Dijk and Bruijnzeel, 2001; Lloyd et al., 1988; Lopes et al., 2020; Schellekens et al., 1999) based on simple assumptions and parameterization methods to describe the interception, storage and redistribution of rainfall in the canopy layer through mathematical formulas. The Gash model can be described as (Cuartas et al., 2007):

$$I_{N} = \begin{cases} c \sum_{i=1}^{m} P_{G}, \ P_{G} < P_{G}' \\ \sum_{i=1}^{n} (I_{W} + I_{S} + I_{A} + I_{T}), \ P_{G} \ge P_{G}' \end{cases}$$
 (5)

Where I_N is the rainfall interception (mm); I_W is the rainfall interception during canopy wetting (mm); I_S is the rainfall interception during saturated canopy conditions (mm); I_A is the

evaporation after rain ceased (mm) (Lopes et al., 2020); I_T is the amount of stem evaporation; P_G is the total amount of precipitation (mm) for a rainfall event and P_G is the amount of water required to completely saturate the canopy (mm) during a rainfall event; m and n are the number of storms insufficient and sufficient to saturate the canopy.

$$I_W = c(P_G' - S_C) \tag{6}$$

$$I_S = c\overline{E_c}/\overline{R}(P_G - P_G') \tag{7}$$

$$I_A = cS_C \tag{8}$$

$$I_T = \begin{cases} 0, \ P'_G < P''_G \\ S_t + P_t P_G, \ P'_G \ge P''_G \end{cases} \tag{9}$$

Where $S_C=S/c$, S is the same as in Rutter; S_t and P_t represent the evaporation storage capacity from trunks and the fraction of incident rainfall that is diverted to the trunks, and the optimization range of these two parameters refers to the experimental results of Cuartas and Lloyd (Cuartas et al., 2007; Lloyd et al., 1988) in this study; c describes the radiation transmittance through crop canopies as an exponential-type attenuation process:

$$c = 1 - \exp(-\kappa LAI) \tag{10}$$

Where κ and LAI are the extinction coefficient and the leaf area index (m²/m²).

In the part of I_S , $\overline{E_c} = \overline{E}/c$, \overline{E} is the ratio of mean evaporation rate (mm/hour); \overline{R} represent the mean rainfall rate (mm/hour). Finally, $P_G^{'}$ and $P_G^{''}$ is the threshold value required to saturate the canopy and the trunk (mm), which can be described as (Gash et al., 1995; Limousin et al., 2008):

$$P_G' = \left(-\frac{\bar{R}}{\bar{E}_C}\right) S_C \ln\left(1 - \frac{\bar{E}_C}{\bar{R}}\right) \tag{11}$$

$$P_G^{\prime\prime} = \left(\frac{\bar{R}}{\bar{R} - \overline{E}_C}\right) (S_t / P_t) + P_G^{\prime} \tag{12}$$

Table S2
The optimized parameters of the models.

Model	Parameter	Unit	Value
	S	mm	1.049
	s _t	-	0.06
Rutter and Gash	p _t	-	0.013
	p	-	0.031

For the Rutter and Gash canopy interception models, the objective is to minimize the difference in annual canopy interception ratio (the ratio of total annual canopy interception to total annual precipitation) from the observation. The parameter optimization for the Rutter and Gash models references the study by Cuartas (Cuartas et al., 2007), which determined an annual average canopy interception rate of 16.5% for the K34 site from 2002 to 2004 through experiments. Although the period used in our study spans from 2002 to 2006, we can still utilize this observational conclusion.

Referances

Borma, L.S., da Rocha, H.R., Cabral, O.M., von Randow, C., Collicchio, E., Kurzatkowski, D., Brugger, P.J., Freitas, H., Tannus, R., Oliveira, L., Rennó, C.D., Artaxo, P., 2009. Atmosphere and hydrological controls of the evapotranspiration over a floodplain forest in the Bananal Island region, Amazonia. J. Geophys. Res. Biogeosciences 114. https://doi.org/10.1029/2007JG000641

Carswell, F.E., Costa, A.L., Palheta, M., Malhi, Y., Meir, P., Costa, J. de P.R., Ruivo, M. de L., Leal, L. do S.M., Costa, J.M.N., Clement, R.J., Grace, J., 2002. Seasonality in CO2 and H2O flux at an eastern Amazonian rain forest. J. Geophys. Res. Atmospheres 107, LBA 43-1-LBA 43-16. https://doi.org/10.1029/2000JD000284

Cuartas, L.A., Tomasella, J., Nobre, A.D., Hodnett, M.G., Waterloo, M.J., Múnera, J.C., 2007. Interception water-partitioning dynamics for a pristine rainforest in Central Amazonia: Marked differences between normal and dry years. Agric. For. Meteorol. 145, 69–83. https://doi.org/10.1016/j.agrformet.2007.04.008

Gan, G., Liu, Y., 2020. Inferring transpiration from evapotranspiration: A transpiration indicator using the Priestley-Taylor coefficient of wet environment. Ecol. Indic. 110, 105853. https://doi.org/10.1016/j.ecolind.2019.105853

Gomis-Cebolla, J., Jimenez, J.C., Sobrino, J.A., Corbari, C., Mancini, M., 2019. Intercomparison of remote-sensing based evapotranspiration algorithms over amazonian forests. Int. J. Appl. Earth Obs. Geoinformation 80, 280–294. https://doi.org/10.1016/j.jag.2019.04.009

Lloyd, C.R., Gash, J.H.C., Shuttleworth, W.J., F, A. de O.M., 1988. The measurement and modelling of rainfall interception by Amazonian rain forest. Agric. For. Meteorol. 43, 277–294. https://doi.org/10.1016/0168-1923(88)90055-X

Morillas, L., Leuning, R., Villagarcía, L., García, M., Serrano-Ortiz, P., Domingo, F., 2013. Improving evapotranspiration estimates in Mediterranean drylands: The role of soil evaporation. Water Resour. Res. 49, 6572–6586. https://doi.org/10.1002/wrcr.20468

Pollard, D., Thompson, S.L., 1995. Use of a land-surface-transfer scheme (LSX) in a global climate model: the response to doubling stomatal resistance. Glob. Planet. Change 10, 129–161. https://doi.org/10.1016/0921-8181(94)00023-7

Restrepo-Coupe, N., Rocha, H.R. da, Hutyra, L.R., Araujo, A.C. da, Borma, L.S., Christoffersen, B., Cabral, O.M.R., Camargo, P.B. de, Cardoso, F.L., Costa, A.C.L. da, Fitzjarrald, D.R., Goulden, M.L., Kruijt, B., Maia, J.M.F., Malhi, Y.S., Manzi, A.O., Miller, S.D., Nobre, A.D., Randow, C. von, Sá, L.D.A., Sakai, R.K., Tota, J., Wofsy, S.C., Zanchi, F.B., Saleska, S.R., 2013. What drives the seasonality of photosynthesis across the Amazon basin? A cross-site analysis of eddy flux tower measurements from the Brasil flux network. Agric. For. Meteorol. 182–183, 128–144. https://doi.org/10.1016/j.agrformet.2013.04.031

Rocha, H., Freitas, H., Rosolem, R., Juárez, R., Tannus, R., Ligo, M., Cabral, O., Dias, M., 2002. Measurements of CO2 exchange over a woodland savanna (Cerrado Sensu stricto) in southeast Brasil. Biota Neotropica 2, 1–11. https://doi.org/10.1590/S1676-06032002000100009

Santos, S.N.M., Costa, M.H., 2004. A simple tropical ecosystem model of carbon, water and energy fluxes. Ecol. Model. 176, 291–312. https://doi.org/10.1016/j.ecolmodel.2003.10.032

Zhang, Y., Kong, D., Gan, R., Chiew, F.H.S., McVicar, T.R., Zhang, Q., Yang, Y., 2019. Coupled estimation of 500 m and 8-day resolution global evapotranspiration and gross primary

production in 2002–2017. Remote Sens. Environ. 222, 165–182. https://doi.org/10.1016/j.rse.2018.12.031

Lloyd, C.R., Gash, J.H.C., Shuttleworth, W.J., F, A. de O.M., 1988. The measurement and modelling of rainfall interception by Amazonian rain forest. Agric. For. Meteorol. 43, 277–294. https://doi.org/10.1016/0168-1923(88)90055-X

Schellekens, J., Scatena, F.N., Bruijnzeel, L.A., Wickel, A.J., 1999. Modelling rainfall interception by a lowland tropical rain forest in northeastern Puerto Rico. J. Hydrol. 225, 168–184. https://doi.org/10.1016/S0022-1694(99)00157-2

Cuartas, L.A., Tomasella, J., Nobre, A.D., Hodnett, M.G., Waterloo, M.J., Múnera, J.C., 2007. Interception water-partitioning dynamics for a pristine rainforest in Central Amazonia: Marked differences between normal and dry years. Agric. For. Meteorol. 145, 69 – 83. https://doi.org/10.1016/j.agrformet.2007.04.008

Dijk, A.I.J.M. van, Bruijnzeel, L.A., 2001. Modelling rainfall interception by vegetation of variable density using an adapted analytical model. Part 1. Model description. J. Hydrol. 247, 230–238. https://doi.org/10.1016/S0022-1694(01)00392-4

Limousin, J.-M., Rambal, S., Ourcival, J.-M., Joffre, R., 2008. Modelling rainfall interception in a mediterranean Quercus ilex ecosystem: Lesson from a throughfall exclusion experiment. J. Hydrol. 357, 57–66. https://doi.org/10.1016/j.jhydrol.2008.05.001

Rutter, A.J., Kershaw, K.A., Robins, P.C., Morton, A.J., 1971. A predictive model of rainfall interception in forests, 1. Derivation of the model from observations in a plantation of Corsican pine. Agric. Meteorol. 9, 367–384. https://doi.org/10.1016/0002-1571(71)90034-3

Gash, J.H.C., Lloyd, C.R., Lachaud, G., 1995. Estimating sparse forest rainfall interception with an analytical model. J. Hydrol. 170, 79–86. https://doi.org/10.1016/0022-1694(95)02697-N